17α-estradiol Alleviates High-Fat Diet-Induced Inflammatory and Metabolic Dysfunction in Skeletal Muscle of Male and Female Mice

Authors: Matthew P. Bubak[1], Shivani N. Mann[2], Agnieszka K. Borowik[1], Atul Pranay[1], Albert Batushansky[1,3], Samim Ali Mondal[1], Stephen M. Diodge[1], Arik Davidyan[1], Marcelina M. Szczygiel[1], Fredrick R. Peelor III[1], Sandra Rigsby[1], Matle Broomfield[1], Charles I. Lacy[4], Heather C. Rice[4], Michael B. Stout[1,5], & Benjamin F. Miller[1,5]

1. Aging and Metabolism Research Program, Oklahoma Medical Research Foundation, Oklahoma City, OK, USA

2. Department of Neuroscience, University of Arizona, Tucson, AZ, USA

3. Ilse Katz Institute for Nanoscale Science & Technology, Ben-Gurion University of the Negev, Beer-Sheba, 8410501, Israel

4. Department of Biochemistry and Molecular Biology, Oklahoma Center for Geroscience & Healthy Brain Aging, Oklahoma City, OK, USA

5. Oklahoma City Veterans Affairs Medical Center, Oklahoma City, OK, USA

Key Words: Estrogen, Metabolism, Obesity, Deuterium Oxide, Lipids

Corresponding Author:

Benjamin F Miller

Benajmin-Miller@omrf.org

Aging and Metabolism Research Program

Oklahoma Medical Research Foundation

825 NE 13th Street

Oklahoma City, Oklahoma 73104

Abstract:

Skeletal muscle has a central role in maintaining metabolic homeostasis. 17α-estradiol (17α-E2), a naturally-occurring non-feminizing diastereomer of 17β-estradiol that demonstrates efficacy for improving metabolic outcomes in male, but not female, mice. Despite several lines of evidence showing that 17α-E2 treatment improves metabolic parameters in middle-aged obese and old male mice through effects in brain, liver, and white adipose tissue little is known about how 17α-E2 alters skeletal muscle metabolism, and what role this may play in mitigating metabolic declines. Therefore, this study aimed to determine if 17α-E2 treatment improves metabolic outcomes in skeletal muscle from obese male and female mice following chronic high fat diet (HFD) administration. We hypothesized that male, but not female, mice, would benefit from 17α-E2 treatment during HFD. To test this hypothesis, we used a multi-omics approach to determine changes in lipotoxic lipid intermediates, metabolites, and proteins related to metabolic homeostasis. In male mice, we show that 17α-E2 alleviates HFD-induced metabolic detriments of skeletal muscle by reducing the accumulation of diacylglycerol (DAGs) and ceramides, inflammatory cytokine levels, and reduced the abundance of most of the proteins related to lipolysis and beta-oxidation. In contrast to males, 17α-E2 treatment in female mice had little effect on the DAGs and ceramides content, muscle inflammatory cytokine levels, or changes to the relative abundance of proteins involved in beta-oxidation. These data support to the growing evidence that 17α-E2 treatment could be beneficial for overall metabolic health in male mammals.

Key Words: Metabolism, Deuterium Oxide, Omics, Obesity**,** Sex Effects

Introduction

Metabolic syndrome is a cluster of conditions that includes obesity, dyslipidemia, hypertension, and insulin resistance.[1,2] Skeletal muscle has a central role in maintaining metabolic homeostasis as it accounts for approximately 70-85% of insulin-stimulated glucose disposal[3,4] and is the primary tissue responsible for oxidative metabolism. Ectopic lipid accumulation in skeletal muscle can lead to metabolic inflexibility[5] and the accumulation of metabolic byproducts such as diacylglycerol (DAG) and ceramides.[6] DAG and ceramides interfere with insulin signaling transduction in skeletal muscle[7,8] and negatively impact whole-body metabolic homeostasis.[9] Strategies such as caloric restriction and exercise modulate nutrient-sensing pathways to prevent and/or reverse age- and obesity-related metabolic dysfunction. [10–13] However, these strategies are often difficult to maintain due to existing comorbidities.[14,15]

17α-estradiol (17α-E2) is a naturally-occurring non-feminizing diastereomer of 17β-estradiol. 17α-E2 supplementation extends median lifespan in male mice when administered during middle[16,17] or advanced ages[18]. We and others have shown that 17α-E2 supplementation in obese and aged male mice reduces caloric intake, ectopic lipid accumulation, regional adiposity, resulting in greater glucose tolerance and insulin sensitivity.[19–23] 17α-E2-mediated declines in caloric intake are not necessary for improvements in metabolic parameters,[20] which suggests that 17α-E2 modulates metabolism through multiple mechanisms[24–27]. Female mice with intact ovarian function do not respond to 17α-E2.[24–30] However, female mice with metabolic dysfunction[31] or that undergo ovariectomy do gain metabolic benefits from 17α-E2.[32] Even so, chronic administration of 17α-E2 does not protect ovariectomized female mice against age-related metabolic dysfunction.[24–27,30] Although it is known that 17α-E2 treatment improves metabolic parameters in some tissues of male mice, little is known about skeletal muscle metabolism in either sex.

It is not clear if the benefits of 17α-E2 treatment on skeletal muscle insulin sensitivity is a direct effect on muscle. What we know about muscle is that 17α-E2 attenuates age-related muscle loss in male, but not female mice.[30] Further, 17α-E2 treatment starting mid-life in male mice increased skeletal muscle amino acid abundance and attenuated skeletal muscle functional declines without altering mTORC1 signaling.[30] We showed that 17α-E2 does not affect skeletal muscle cellular proliferation and proteostatic maintenance when

administered late-in-life,[19] which supports that 17α-E2 elicits benefits through mTOR-independent mechanisms.

This study aimed to determine if 17α-E2 treatment improves metabolic and proteomic outcomes in skeletal muscle of male and female mice fed a HFD. We hypothesized that male, but not female mice, would benefit from 17α-E2 treatment during HFD with remodeling of the mitochondrial proteome to support lipid oxidation and reductions in DAG and ceramide content. Unexpectedly, 17α-E2 had marked but different beneficial effects within each sex that point to differing mechanisms of action between male and female rodents.

1. Methods

1.1 Ethical Approval and Study Design

Resources are provided in **Supplementary Table 1**. The Institutional Animal Care and Use Committee of the Oklahoma City VA reviewed and approved all animal procedures. These animals were part of a larger study published elsewhere.[31] We reproduce body and fat mass from the previous publication because they inform our analyses. We bred experimental C57BL/6 mice in-house, group-housed by sex and fed standard chow until 12 weeks of age. At 12 weeks of age, mice (except chow) were fed a HFD for 39 weeks. We individually housed mice two weeks prior to study initiation and kept on a 12:12-hour light-dark cycle. Mice had ad libitum access to food and water. At 12 months of age, one HFD group began 17α-E2 at 14.4 ppm (HFD+17α-E2) for 14-weeks. We measured body mass and composition (EchoMRI, Houston, TX) weekly. We labeled mice with deuterium oxide (D_2O) 10 days prior to sacrifice according to previously published methods.[19,33] At 14-weeks post treatment, mice were fasted for 5-6 hours and euthanized via cardiac puncture with blood collected into EDTA-lined tubes on ice, and immediately frozen. Lower limb skeletal muscles were removed, weighed, flash frozen, and stored at -80°C. One gastrocnemius was fixed in 4% paraformaldehyde, cryo-embedded, and stored at -80°C.

1.2 Determination of cellular signaling

For cellular signaling, we isolated the cytosolic fraction from 20–30 mg of homogenized quadriceps. We determined protein concentration using Peirce 660 assay as described previously[34]. Western fractions were processed by the ProteinSimple WES system (San Jose, CA, USA).

1.3 Skeletal muscle lipid assessments

We used three approaches to assess skeletal muscle lipid species. We assessed total muscle lipids with Oil-Red-O (ORO) on one gastrocnemius embedded in OCT (ThermoFisher, Walham, MA) and cryosectioned into 10 µm sections[35]. Brightfield images were taken on a Zeiss 710 confocal microscope (Oberkochen, Germany), tiled, stitched at 20x and imaged (ImageJ) at a threshold of 0-172.

For total muscle triacylglycerol content, we homogenized 100 mg of quadriceps in 10X (v/w) Cell Signaling Lysis Buffer (Cell Signaling, Danvers, MA) with phosphatase and protease inhibitors (Boston BioProducts, Boston, MA). Total lipid was extracted using the Folch method[36] and dried with nitrogen prior to reconstitution in 100 µL of 3:1:1 tert-butyl alcohol-methanol-Triton X-100 solution. We determined triacylglycerol concentrations using a spectrophotometric assay with a 4:1 Free Glycerol Agent / Triacylglycerol Agent solution.[37]

Finally, we assessed individual lipid species in 25 mg of powdered gastrocnemius using a lipidomic approach through the NORC Lipidomics Core Laboratory at the University of Colorado-Denver on HPLC-MS/MS[38]. We determined the concentrations of 1,2-diacylglycerols (1-2-DAG), 1,3-diacylglycerols (1-3-DAG), total ceramides (Cer), dihydroceramides (dhCer), 1-O-glucosylceramides (GluCer), 1-O-lactosylceramides (LacCer), and 1-O-galactosylceramides (GlaCer).

1.4 Skeletal muscle inflammation

We used two approaches to determine skeletal muscle inflammation. First, total RNA was extracted from 20-30 mg of homogenized tibalis anterior (TA) via Trizol (Life Technologies, Carlsbad, CA) and reverse transcribed to cDNA using the High-Capacity cDNA Reverse Transcription kit (Applied Biosystems, Foster City, CA). Real-time PCR was performed in a QuantStudio 12K Flex Real Time PCR System (Thermofisher Scientific, Waltham, MA) using TaqMan™ Gene Expression Master Mix (Applied Biosystems/Thermofisher Scientific, Waltham, MA) and predesigned gene expression assays with FAM probes (Integrated DNA Technologies, Skokie, Illinois). Expression of IL-6, IL-1α, and TNFα (ThermoFischer, Waltham, MA) was expressed as $2^{-\Delta\Delta CT}$ by the comparative CT method[39] and normalized to the expression of HGPRT (ThermoFischer, Waltham, MA).

Second, we assessed concentrations of cytokines in TA muscle lysate using V-PLEX Mouse Proinflammatory Panel I immunoassays using manufacturers instructions. We normalized the concentrations of IFN-γ, IL-10, IL-12p70, IL-1β, IL-2, IL-4, IL-5, IL-6, KC/GRO, and TNF-α to total protein concentration.

1.5 Assessment of skeletal muscle metabolites

We used semi-targeted metabolic profiling for glycolysis, amino acids, and TCA cycle metabolites using an Agilent 7890B gas chromatograph coupled to a 5977A mass spectrometer as previously published[40]. Samples were randomized and analyzed in two batches and the metabolites relative abundance was calculated by peak area followed by normalization with sample weight and total ion current (TIC) median. The data from two batches were combined for analysis using integrated exploratory approach to remove the batch effect using 'limma' package for R.[41]

1.6 Assessments of protein turnover and content

We determined protein synthesis of myofibrillar and mitochondrial proteins on 20 mg of quadriceps skeletal according to our previously published procedures.[41–45] For relative abundance of individual proteins, we performed proteomic analysis on 20 µg of gastrocnemius as previously described [46,47].

1.7 Statistical Analyses

We examined responses within a sex, but not between sexes. Within each sex we used a one-way ANOVA (Graphpad Prism 9, San Diego, CA, USA) and R with packages "dplyer", hmisc", and "stringer" unless otherwise stated. For changes in body composition over the 12 weeks of treatment (**Figure 2A-2F**), we used a two-way ANOVA (treatment x time). For the lipid analysis, outliers were removed using R package "Routliers" and mean absolute deviation function.[48,49] A Tukey post-hoc analysis was run to determine where differences occurred. For lipid analysis, lipids that were different were explored for their biological relationships using Human Metabolome Data Base and LIPID MAPS Structure Data Bases.[50] For metabolite abundance the one-way ANOVA was performed on Log10-transformed normalized data with R-environment. For proteomics, shared peptides within a group, which we defined as being identified within 50% of the samples, were considered for further analysis of proteins and their biological relationships using Uniprot, Gene Ontology (GO), and PANTHER databases and using R programming language (3.4.0) and "dplyer" package.[48] On Log10-transformed normalized data we performed an unsupervised principal component analysis (PCA) using the online tool based on R packages 'stats' and 'heatmap2'.[51] Results are presented as mean ± standard error (SE) with *p* values less than 0.05 considered to be significant.

2. **Results**

2.1 Body Composition

As shown elsewhere,[31] body mass and fat mass were found to have a main effect of time and treatment for male mice, and a main effect of treatment in female mice. For fat-free mass, there was a main effect of treatment for male mice, and a main effect of time in the female mice. In male mice, body mass, fat mass and lean mass changed over time (interaction effect, **Figure 2A-C**). In female mice, there was an interaction for body mass and fat mass (**Figure 2D-F**). When expressed as percent change, both male and female 17α-E2+HFD had a higher percent lean mass than HFD (**Figure 2G**); in male, but not female mice, 17α-E2+HFD had a lower percent lean mass than Chow (**Figure 2G**). In the male mice, the HFD had lower relative muscle masses when normalized to body mass in the quadriceps and gastrocnemius compared to the Chow and HFD+17α-E2, while the Chow had greater masses compared to the HFD+17α-E2 (**Figure 2H and 2J**). Additionally, in male mice the tibialis anterior had greater mass in the Chow compared to the HFD and HFD+17α-E2 (**Figure 2I**). Lastly, in male mice the soleus was greater in the Chow compared to the HFD (**Figure 2K**). In female mice the quadriceps, gastrocnemius, and soleus have lower relative masses in the HFD compared to the Chow and HFD+17α-E2 groups (**Figure 2H, J, and K**). Additionally in the female mice, the HFD had lower relative muscle masses when normalized to body mass in the tibialis anterior compared to the Chow and HFD+17α-E2, while the Chow had greater masses compared to the HFD+17α-E2 (**Figure 2I**). However, there was little effect of treatment in both male and female mice when normalized to tibia length (**Supplemental Figure 1**).

2.2 AMPK and mTOR signaling

In the male mice, we saw an increase in pAMPK/total levels in the HFD+17α-E2 compared to Chow and HFD, but no difference in female mice (**Figure 3)**. However, female undergoing 17α-E2 treatment had a lower p-AKT/total ratio than the Chow. These data show that 17α-E2 had little effect on downstream targets of mTOR pathway and AMPK signaling (**Figure 3 and Supplemental Figure 2**).

2.3 Muscle lipid-related outcomes

Male HFD had greater in OROO staining than Chow and a trend toward greater staining in the HFD+17α-E2 compared to Chow (**Figure 4A and B**). Female HFD+17α-E2 was greater than Chow, with a trend toward higher concentration in HFD versus Chow (**Figure 4A and B**). Compared to Chow, male HFD and HFD+17α-E2 had higher quadriceps triacylglycerol concentration (**Figure 4C**). In female mice, HFD had higher triacylglycerol concentration than both Chow and HFD+17α-E2 (**Figure 4C**).

In the gastrocnemius of male mice, there were greater total 1,2-DAGs and 1,3-DAGs in HFD versus Chow, while HFD+17α-E2 was less than HFD for both (**Figure 4D**). In contrast, there were no differences in female mice across the majority of total saturated, unsaturated, monounsaturated, and polyunsaturated FAs (**Supplemental Figures 3-9**). When presented as a heat map, there are striking differences between male and female mice in how HFD and HFD+17α-E2 change 1,2-DAG profiles (**Figure 4E**). Additionally, there appears to be changes that are specific to male or female mice and the direction of those changes in six lipid species (**Figure 4E**). The Human Metabolite Data Base showed that these six DAGs are intermediates for plasmalogen synthesis, de novo triacylglycerol synthesis, and beta-oxidation of long chain fatty acids (**Supplemental table 2 and 3**). There were no changes with treatment in total ceramides for male and female mice (**Supplemental Figure 5**). When broken down by subclasses of ceramides, HFD male mice had greater total and unsaturated dhCeramides and LacCeramides compared to Chow and HFD+17α-E2 (**Supplemental Figure 6 and 9**).

2.4 <u>Skeletal muscle inflammation</u>

Our results show that the male HFD mice had greater mRNA expression of IL-6, IL-1α, and TNFα compared to the Chow and HFD+17α-E2 (**Figure 5A**). There were no differences in female mice (**Figure 5A**). When examining cytokine concentrations, male HFD had greater concentration of IL-10 compared to Chow and HFD+17α-E2, while the HFD+17α-E2 was greater than Chow. The male HFD had greater concentration of IL-12p70 and KCGRO compared to Chow, less IL-6 concentration compared to Chow, and HFD+17α-E2 had lower TNFα concentrations compared to HFD. In the female mice, the HFD had greater concentration of IL-10 compared to Chow and HFD+17α-E2. Also, the female HFD+17α-E2 had a greater IL-6 concentration compared to Chow. There were no differences among the groups for IFNγ, IL-1B, IL-2, IL-4, IL-5 in male or

female mice and no differences in TNFα or IL-12p70 in the female mice (**Figure 5B** and **Supplemental Figure 10**). IFNγ and IL-4 were below the detection range of the stand curve (**Supplemental Figure 10**).

2.5 Skeletal muscle metabolites

Across the principal component 1 (PC_1), there was a separation based on diet between the Chow versus HFD and HFD+17α-E2 (regardless of 17α-E2) in male mice, but a smaller separation of HFD and HFD+17α-E2. Across PC_2, there is a small separation between the HFD and HDF+17α-E2, however, only a small percentage of the variance is explained by 17α-E2 (**Figure 6A**). Conversely, female groups were not clearly separated (**Figure 6B**). Our results show that HFD and HFD+17α-E2 had greater alanine, succinic acid, and serine abundance in both male and female mice compared to Chow, while glycine, beta alanine, aminomalonic acid and adenosine were altered in abundance in response to HFD and HFD+17α-E2 in male mice only (**Figure 6C and Supplemental Figure 11**). Tyrosine was elevated in the HFD compared to the HFD+17α-E2 in female mice (**Figure 6D**). The female HFD mice had a greater abundance of taurine and tyrosine compared to Chow (**Figure 6D and Supplemental Figure 11**). However, there were only three metabolites glucose-6-phosphate, threonine, and succinic acid that were different in the HFD compared to the HFD+17α-E2 in male mice (**Figure 6C, Supplemental Figure 11**). Glucose-6-phosphate and threonine were lower in HFD compared to HFD+17α-E2 in male mice while succinic acid was higher in HFD compared to HFD+17α-E2 (**Figure 6C and Supplemental Figure 11**). We did not observe similar change in these metabolites between HFD and HFD+17α-E2 in female mice (**Figure 6D and Supplemental Figure 11**).

2.6 Protein turnover and proteomic analysis

In the quadriceps, the myofibrillar fractional synthesis rate (FSR) was greater in the HFD and HFD+17α-E2 compared to Chow of male mice. There were no differences in the myofibrillar FSR among the female mice (**Figure 7A**). In the mitochondrial fraction, the male mice had greater FSR in the HFD and HFD+17α-E2 compared to Chow. The female HFD mice had greater mitochondrial FSR compared to the Chow and HFD+17α-E2 (**Figure 7B**).

In the male mice, the PCA plot shows limited clustering among the groups. HDF+17α-E2 partially clusters with the HFD, thus 17α-E2 explains a low amount of variance (**Figure 7C**). In female mice, the PCA shows no clear separation (**Figure 7D**). In male mice, the relative abundance of 52 of 618 identified proteins were significantly different (>log2-fold change of 1.3) in the HFD+17α-E2 compared to HFD, while in the female mice 26 of 586 identified proteins were significantly different in the HFD+17α-E2 compared to HFD (**Figure 7E and 7F**). Of the 52 proteins identified in the male mice, 20 were involved in mitochondrial and beta oxidation processes, 17 were structural and/or contractile proteins, nine were related to synthetic processes, and seven had other biological functions. In female mice, of the 26 proteins identified eight were involved in mitochondrial and beta oxidation processes, three were structural and/or contractile proteins, five were related to synthetic processes, and 10 had other biological functions. The abundance and primary functions of the significantly different individual proteins are listed in **Supplementary table 4.** HFD+17α-E2 had greater abundance of mitochondrial proteins involved in the mitochondrial membrane ATP synthase and the oxidization of long chain fatty acids, carbohydrates and amino acids (ADHX, ODO1, and ATPB) compared to HDF. Interestingly, there was also a greater abundance of proteins involved in mitochondrial membrane ATP synthase and NADH dehydrogenase (NDUA8 ATOP, and ATP5L) in the HFD+17α-E2 compared to HFD (**Figure 7E**). These significantly different proteins were grouped by GO terms and the enriched pathways involved ATP metabolic process (GO:0046034), oxidative phosphorylation (GO:0006119), proton motive force-driven mitochondrial ATP synthesis (GO:0042776), and carbohydrate catabolic process (GO:0016052, **Supplementary table 5**). In female HFD+17α-E2 mice there was a reduced abundance of mitochondrial-related proteins (6 of 7) such as those involved in beta-oxidation and ATP synthesis (DECR and ADT1) and a great abundance of NDUA4, a component of the cytochrome c oxidase which drives oxidative phosphorylation, in the HFD+17α-E2 compared to HFD (**Figure 7F**). These proteins are involved in energy production and beta oxidation; thus it appears that 17α-E2 treatment alters mitochondrial beta oxidation and skeletal muscle metabolism. There was no enrichment in biological pathways for female mice.

3. **Discussion**

We tested the hypothesis that 17α-E2 would be protective against HFD-induced metabolic derangements in skeletal muscle of male, but not female, mice. As reported elsewhere,[31] 17α-E2 improves body composition in

both sexes, but also improves metabolic parameters in the skeletal muscle of male mice on a HFD. 17α-E2 alleviates HFD-induced metabolic detriments of skeletal muscle by reducing the accumulation of bioactive lipids, inflammatory cytokines, and the abundance of most of the proteins related to lipolysis and beta-oxidation. In contrast to males, 17α-E2 in female mice had little effect on the muscle inflammatory status, the majority of bioactive lipid intermediates, or changes to the relative abundance of proteins involved in beta-oxidation. These data further support that 17α-E2 treatment could be beneficial for overall metabolic health in male mammals.

The expansion of lipid storage in adipose tissue leads to the release of pro-inflammatory cytokines[52] and ectopic lipid storage in skeletal muscle.[53] This storage of lipids in muscle can lead to impairment of insulin-stimulated glucose uptake,[54] contributing to overall insulin resistance. We explored whether the beneficial effects of 17α-E2 treatment on insulin sensitivity in male mice were partly due to improvements in skeletal muscle. To ensure an obese phenotype in the mice, we administered a HFD for approximately 9 months prior to treatment with 17α-E2. As was our goal, the male mice had approximately double the fat mass compared to chow when starting 17α-E2 treatment. Although lean mass was slightly increased in the HFD at the start of treatment, the percentage lean mass was greater at the end of treatment. Therefore, there was less lean mass, and potentially muscle mass, to help maintain metabolic flexibility. After 12 weeks of 17α-E2 treatment, there were improvements in percent lean mass despite continued HFD, supporting previous studies in male mice.[21,23] Although there were minimal differences in absolute muscle masses (**Supplemental Figure 1**) at the end of the treatment period, the muscle mass normalized to body mass was significantly improved with 17α-E2 treatment (**Figure 1H-K**), thus improving the potential to maintain metabolic flexibility.

The HFD increased ectopic lipid deposition in male mice as evidenced by higher ORO staining and muscle triglycerides. Under low flux conditions, as with sedentary behavior, incomplete oxidation of triacylglycerol via lipases results in the accumulation of bioactive lipid metabolites such as DAGs and ceramides.[7] These lipid intermediates are thought to mediate of lipid-induced insulin resistance.[8,9,55] Consistent with this idea, the higher levels of triglycerides in male mice were matched by higher overall levels of DAGs, but not ceramides. Our lipidomic analyses showed that both 1,2- and 1,3-DAGs were higher with HFD compared to chow. In

addition, the DAG 18:0, which is linked to insulin resistance,[56] was elevated with HFD in male mice. In the male mice, these changes in lipid species were associated with significantly higher expression of the pro-inflammatory cytokines IL-6, IL-1α, and TNFα, which are linked to whole-body insulin sensitivity.[57] Interestingly, IL-10, which is an anti-inflammatory cytokine, was elevated in both sexes on the HFD which is likely due to compensatory mechanisms. Treatment with 17α-E2 during HFD had several interesting changes to lipids in skeletal muscle. The most striking was that even though total lipids and triglycerides remained higher than Chow, there was a significant decrease in 1,2- and 1,3-DAGs, including 18:0, compared to HFD. These differences were matched by significantly lower expression of IL-6 and IL-1α. These findings support that 17α-E2 in male mice has positive changes in lipid profiles in skeletal muscle, potentially improving insulin sensitivity.

Our findings in female mice were partially unexpected. First, treatment with 17α-E2 completely reversed the HFD-induced increase in fat mass so that there were no longer differences compared to Chow. Like male mice, 17α-E2 treatment resulted in higher percentages of lean mass and muscle mass normalized to body mass. With HFD, female mice had significantly greater muscle triglycerides and a trend ($p=0.06$) toward higher total lipids. Unlike male mice, HFD in female mice did not increase 1,2- or 1,3-DAGs or expression of any pro-inflammatory cytokines. In addition, the muscle concentration of cytokines, which would likely include contributions from the systemic environment, also showed minimal changes with HFD in female mice. It is thought that compared to male adipose tissue, female adipose tissue has a greater capacity to expand and store lipids thus minimizing ectopic lipid stored.[58] Although our data showed increased lipids in female muscle, it is tempting to speculate that high turnover was maintained in the lipid pools, thus minimizing the accumulation of DAGs. HFD+17α-E2 had lower muscle triglyceride levels compared to HFD, but there were no changes to DAGs or cytokines expression in muscle because they were not greater with HFD to begin with. Therefore, our data showed some overall benefits on body composition of female mice on a prolonged HFD, but there were minimal improvements in muscle because the muscle was remarkably resistant to HFD-induced changes.

There is one more interesting finding with the regard DAGs that is worth noting. There were six 1,2-DAG species (18:0/18, 18:1, 18:0, 18:0/22, 16:0/20, and 18:0/20) that had essentially opposite responses to HFD and 17α-E2 treatment. These species were higher in the male HFD compared to Chow but were not different from Chow with HFD+17α-E2. In female HFD, these species were not different between Chow and HFD, but were greater with HFD+17α-E2. While in male mice these changes mirror those of other 1,2-DAGs, in female mice they are the only ones that increased with 17α-E2 treatment. According to the Human Metabolome Data Base, these six 1,2-DAGs are involved in de novo triacylglycerol biosynthesis, plasmalogen synthesis, and mitochondrial beta-oxidation of long-chain saturated fatty acids (**supplementary tables 2 and 3**).

We wanted to determine if changes in lipid deposition and inflammation impacted muscle metabolism. To do so, we used a semi-targeted metabolomic profiling approach that focused on 45 metabolites. From our PCA, we saw that male mice clearly separate by Chow versus HFD, while female mice had no separation. Interestingly, 17α-E2 treatment did not result in any further separation in male mice. We focused on amino acid concentrations because a previous study showed that in aged male mice, 17α-E2 had greater skeletal muscle amino acid abundance compared to controls while the inverse was true in aged female mice.[30] Although we found some changes in amino acids concentrations in both sexes, the changes were not unidirectional or consistent with HFD and HFD+17α-E2, limiting our ability to make broad conclusions about the impacts on amino acid metabolism.

In male mice, HFD+17α-E2 had increased AMPK activation compared to both Chow and HFD. A previous study in male mice without HFD showed no changes in AMPK activation of skeletal muscle, although there was an increase in white adipose tissue.[21] AMPK activation is thought to be a primary mechanism of the improvements in insulin sensitivity by the anti-diabetic drug metformin.[59] In the case of metformin, this results in a lowering of hepatic glucose output and improvements in glucose uptake in muscle.[60–62] Although inhibition of mTOR often follows activation of AMPK, we did not find any changes in mTOR signaling in the muscle of male or female mice. This finding further supports the notion that the positive effects of 17α-E2 are mTOR-independent unlike other healthspan-extending treatments.[21,24,30]

Previously, we examined the impact of 17α-E2 on protein turnover in older mice.[19] In that study, there was a lack of changes in protein turnover, although a group that was pair-fed to be deficient in calories equal to the reduced intake from 17α-E2 treatment did have changes in protein turnover. In the current study, male mice had greater myofibrillar protein synthesis with HFD as we have demonstrated previously.[63,64] Surprisingly, there was not an increase in mTOR signaling that is often present in skeletal muscle with obesity. It is important to note that the measurements of protein synthesis were made after months of Chow or HFD and in the last 2 weeks of a 12-week 17α-E2 treatment. Therefore, at this point, lean mass had stabilized, and the synthesis rates likely indicative a steady state and not acute remodeling. If protein synthesis is higher, and lean mass and muscle masses are maintained, there must also be a higher rate of protein breakdown. This higher turnover rate would indicate improved maintenance of proteostasis in the HFD+17α-E2. There was also an increase in mitochondrial protein synthesis with HFD in male mice. We have shown increases in mitochondrial protein synthesis during HFD,[63,65,66] but these studies are shorter in duration and thought to be compensatory changes from the diet. Interestingly, rates of mitochondrial protein synthesis were also higher in the HFD+17α-E2 group. Our proteomic analysis showed extensive differences in the mitochondrial proteome between HFD and HFD+17α-E2 group. Therefore, although both HFD and HFD+17α-E2 had greater mitochondrial protein FSR than Chow, these rates are resulting in different proteins; likely compensatory to HFD in one case, and corrective in the other. This speculation is supported by a lower relative abundance of the majority of individual mitochondrial proteins involved in beta-oxidation and energy production in HFD+17α-E2 compared to HFD (**Figure 8B, supplemental table 4 and 5**); many of which are downstream of ERα signaling.[67–70]

In female mice, the HFD did not increase myofibrillar protein synthesis. As far as we are aware, this is the first study demonstrating this difference between the sexes in myofibrillar protein synthesis rates to HFD. This finding also adds to the overall picture that skeletal muscle of female mice is protected from HFD-induced detriments. As opposed to myofibrillar protein synthesis, the mitochondrial protein synthesis was higher than chow with HFD. When female mice had 17α-E2 during HFD, the mitochondrial protein synthesis was not different from Chow. Since our proteomics analysis also showed a dearth of changes in mitochondria-related protein abundance between HFD and HFD±17α-E2, there was likely no substantive differences with treatment,

perhaps because none were needed. With treatment, there was a reduction in body and fat mass of female mice and no differences in triglycerides concentrations, DAG or ceramide content, or inflammatory cytokines between the Chow and HFD+17α-E2. Therefore, we speculate that the female mouse muscle is resistant to detrimental effects of HFD, thus not deriving muscle-specific benefits from 17α-E2 treatment. There are a couple of limitations to our study. First, we could not assess early changes to treatment with 17α-E2 since we focused on outcomes 12 weeks into treatment. Although we were interested in long-term changes from 17α-E2 treatment, the early changes would be interesting to assess from a remodeling perspective. Second, we did not assess the impact of 17α-E2 concurrent with the onset of HFD. In that sense, we examined 17α-E2's therapeutic potential rather than the potential to prevent HFD-induced changes in metabolism. That said, it is generally thought that reversing conditions is more challenging than prevention, thus demonstrating the great benefits of 17α-E2 treatment. Finally, we were limited in our assessments of metabolic flux. Adding other tracers needed for flux measurements would be challenging analytically because of the planned turnover measurements using D_2O. However, true flux measurements would allow for further understand the positive changes in muscle lipid species.

Our study adds to the growing literature that the healthspan benefits of 17α-E2 are mediated through positive metabolic changes. In the present study we focus on skeletal muscle and show that the positive effects differ between sexes. In male mice, there were direct benefits on the skeletal muscle that resulted in positive changes in lipid species, decreased inflammation, and likely improved remodeling to maintain proteostasis. In female mice, the impact of HFD on skeletal muscle was minimal to begin with, thus 17α-E2 treatment had fewer benefits. However, the 17α-E2 treatment greatly reduced fat mass and likely has other systemic benefits as a result. Therefore, contrary to our hypothesis, 17α-E2 benefit female mice, although these may be minimal directly on skeletal muscle. Future studies will focus on better understanding changes in metabolic flux in skeletal muscle with 17α-E2 treatment.

Funding

Supported by the National Institutes of Health (T32 AG052363 to MPB, S.N.M, and A.D; R00 AG051661 and R01 AG070035 to MBS; P20 GM139763 for AP), and the US Department of Veterans Affairs (Pilot Grant to MBS).

CRediT Authorship Contribution Statement

Conceptualization and study design (SNM, BFM, MBS); data collection (MPB, SNM, SMD, AD, MMS, FRP, SR, MB, CIL), data analysis (MPB, SNM, SMD, AD, MMS, FRP, SR, MB, HCR, CIL), manuscript writing (MPB, SNM, MBS, BFM). All authors reviewed the manuscript and approved the final version.

Conflicts of Interest

There are no conflicts of interest to declare.

Acknowledgements

We acknowledge BioRender.com for images, and the OMRF Center for Biomedical Data Sciences for assistance with bioinformatics and figures.

Data Availability

Data will be shared on reasonable request to the corresponding author.

References:

1. Alberti KG, Zimmet PZ. Definition, diagnosis and classification of diabetes mellitus and its complications. Part 1: diagnosis and classification of diabetes mellitus provisional report of a WHO consultation. *Diabet Med*. 1998;15(7):539-553. doi:10.1002/(SICI)1096-9136(199807)15:7<539::AID-DIA668>3.0.CO;2-S

2. Reaven GM. Role of Insulin Resistance in Human Disease. *Diabetes*. 1988;37(12):1595-1607. doi:10.2337/DIAB.37.12.1595

3. Yki-Järvinen H, Young AA, Lamkin C, Foley JE. Kinetics of glucose disposal in whole body and across the forearm in man. *J Clin Invest*. 1987;79(6):1713-1719. doi:10.1172/JCI113011

4. DeFronzo RA, Jacot E, Jequier E, Maeder E, Wahren J, Felber JP. The Effect of Insulin on the Disposal of Intravenous Glucose: Results from Indirect Calorimetry and Hepatic and Femoral Venous Catheterization. *Diabetes*. 1981;30(12):1000-1007. doi:10.2337/DIAB.30.12.1000

5. Goodpaster BH, Wolf D. Skeletal muscle lipid accumulation in obesity, insulin resistance, and type 2 diabetes. *Pediatr Diabetes*. 2004;5(4):219-226. doi:10.1111/J.1399-543X.2004.00071.X

6. Kelley DE, Goodpaster B, Wing RR, Simoneau JA. Skeletal muscle fatty acid metabolism in association with insulin resistance, obesity, and weight loss. *Am J Physiol Endocrinol Metab*. 1999;277(6 40-6). doi:10.1152/AJPENDO.1999.277.6.E1130/ASSET/IMAGES/LARGE/AEND11223004X.JPEG

7. Koves TR, Ussher JR, Noland RC, et al. Mitochondrial Overload and Incomplete Fatty Acid Oxidation Contribute to Skeletal Muscle Insulin Resistance. *Cell Metab*. 2008;7(1):45-56. doi:10.1016/j.cmet.2007.10.013

8. Broskey NT, Obanda DN, Burton JH, Cefalu WT, Ravussin E. Skeletal muscle ceramides and daily fat oxidation in obesity and diabetes. *Metabolism*. 2018;82:118-123. doi:10.1016/j.metabol.2017.12.012

9. Amati F, Dubé JJ, Alvarez-Carnero E, et al. Skeletal muscle triglycerides, diacylglycerols, and ceramides in insulin resistance: another paradox in endurance-trained athletes? *Diabetes*. 2011;60(10):2588-2597. doi:10.2337/db10-1221

10. Masoro EJ. Caloric restriction-induced life extension of rats and mice: a critique of proposed mechanisms. *Biochim Biophys Acta*. 2009;1790(10):1040-1048. doi:10.1016/J.BBAGEN.2009.02.011

11. Guridi M, Kupr B, Romanino K, et al. Alterations to mTORC1 signaling in the skeletal muscle differentially affect whole-body metabolism. *Skelet Muscle*. 2016;6(1):1-14. doi:10.1186/S13395-016-0084-8/FIGURES/6

12. Liu X, Yuan H, Niu Y, Niu W, Fu L. The role of AMPK/mTOR/S6K1 signaling axis in mediating the physiological process of exercise-induced insulin sensitization in skeletal muscle of C57BL/6 mice. *Biochimica et Biophysica Acta (BBA) - Molecular Basis of Disease*. 2012;1822(11):1716-1726. doi:10.1016/J.BBADIS.2012.07.008

13. Bori Z, Zhao Z, Koltai E, et al. The effects of aging, physical training, and a single bout of exercise on mitochondrial protein expression in human skeletal muscle. *Exp Gerontol*. 2012;47(6):417-424. doi:10.1016/J.EXGER.2012.03.004

14. Dirks AJ, Leeuwenburgh C. Caloric restriction in humans: Potential pitfalls and health concerns. *Mech Ageing Dev*. 2006;127(1):1-7. doi:10.1016/J.MAD.2005.09.001

15. Shigaki C, Kruse RL, Mehr D, et al. Motivation and diabetes self-management. *Chronic Illn*. 2010;6(3):202-214. doi:10.1177/1742395310375630

16. Strong R, Miller RA, Antebi A, et al. Longer lifespan in male mice treated with a weakly estrogenic agonist, an antioxidant, an α-glucosidase inhibitor or a Nrf2-inducer. *Aging Cell*. 2016;15(5):872-884. doi:10.1111/acel.12496

17. Harrison DE, Strong R, Allison DB, et al. Acarbose, 17-α-estradiol, and nordihydroguaiaretic acid extend mouse lifespan preferentially in males. *Aging Cell*. 2014;13(2):273-282. doi:10.1111/acel.12170

18. Harrison DE, Strong R, Reifsnyder P, et al. 17-a-estradiol late in life extends lifespan in aging UM-HET3 male mice; nicotinamide riboside and three other drugs do not affect lifespan in either sex. *Aging Cell*. 2021;00:e13328. doi:10.1111/acel.13328

19. Miller B, Pharaoh G, … KHTJ of, 2020 U. Short-term calorie restriction and 17α-estradiol administration elicit divergent effects on proteostatic processes and protein content in metabolically active tissues. *academic.oup.com*. 2020;75(No. 5):849-857.

20. Steyn FJ, Ngo ST, Chen VP, et al. 17α-estradiol acts through hypothalamic pro-opiomelanocortin expressing neurons to reduce feeding behavior. *Aging Cell*. 2018;17(1):e12703. doi:10.1111/acel.12703

21. Stout MB, Steyn FJ, Jurczak MJ, et al. 17A-Estradiol Alleviates Age-Related Metabolic and Inflammatory Dysfunction in Male Mice Without Inducing Feminization. *Journals of Gerontology - Series A Biological Sciences and Medical Sciences*. 2017;72(1):3-15. doi:10.1093/gerona/glv309

22. Sidhom S, Schneider A, Fang Y, et al. 17α-Estradiol Modulates IGF1 and Hepatic Gene Expression in a Sex-Specific Manner. *The Journals of Gerontology: Series A*. 2020;XX(Xx):1-8. doi:10.1093/gerona/glaa215

23. Mann SN, Hadad N, Nelson Holte M, et al. Health benefits attributed to 17α-estradiol, a lifespan-extending compound, are mediated through estrogen receptor α. *Elife*. 2020;9(3):518-528. doi:10.7554/eLife.59616

24. Garratt M, Bower B, Garcia GG, Miller RA. Sex differences in lifespan extension with acarbose and 17-α estradiol: gonadal hormones underlie male-specific improvements in glucose tolerance and mTORC2 signaling. *Aging Cell*. 2017;16(6):1256-1266. doi:10.1111/acel.12656

25. Garratt M, Lagerborg KA, Tsai YM, Galecki A, Jain M, Miller RA. Male lifespan extension with 17-α estradiol is linked to a sex-specific metabolomic response modulated by gonadal hormones in mice. *Aging Cell*. 2018;17(4):1-14. doi:10.1111/acel.12786

26. Garratt M, Stout MB. Hormone actions controlling sex-specific life-extension. *Aging*. 2018;10(3):293-294. doi:10.18632/aging.101396

27. Debarba LK, Jayarathne HSM, Miller RA, Garratt M, Sadagurski M. 17-α-Estradiol Has Sex-Specific Effects on Neuroinflammation That Are Partly Reversed by Gonadectomy. *J Gerontol A Biol Sci Med Sci*. 2022;77(1):66-74. doi:10.1093/gerona/glab216

28. Isola JV V, Zanini BM, Sidhom S, et al. 17α-Estradiol promotes ovarian aging in growth hormone receptor knockout mice, but not wild-type littermates. *Exp Gerontol*. 2020;129(September 2019):110769. doi:10.1016/j.exger.2019.110769

29. Isola JV V, Zanini BM, Hense JD, et al. Mild calorie restriction, but not 17α-estradiol, extends ovarian reserve and fertility in female mice. *Exp Gerontol*. 2022;159(December 2021):111669. doi:10.1016/j.exger.2021.111669

30. Garratt M, Leander D, Pifer K, et al. 17-α estradiol ameliorates age-associated sarcopenia and improves late-life physical function in male mice but not in females or castrated males. *Aging Cell*. 2019;18(2):e12920. doi:10.1111/acel.12920

31. Mondal SA, Mann SN, Van Der Linden C, et al. Metabolic benefits of 17α-estradiol in liver are partially mediated by ERβ in male mice. doi:10.1101/2023.03.25.534216

32. Mann SN, Pitel KS, Nelson-Holte MH, et al. 17α-Estradiol prevents ovariectomy-mediated obesity and bone loss. *Exp Gerontol*. 2020;142(October):111113. doi:10.1016/j.exger.2020.111113

33. Miller BF, Reid JJ, Price JC, Lin HJL, Atherton PJ, Smith K. CORP: The use of deuterated water for the measurement of protein synthesis. *J Appl Physiol*. 2020;128(5):1163-1176. doi:10.1152/japplphysiol.00855.2019

34. Lawrence MM, van Pelt DW, Confides AL, et al. Massage as a mechanotherapy promotes skeletal muscle protein and ribosomal turnover but does not mitigate muscle atrophy during disuse in adult rats. *Acta Physiologica*. 2020;229(3). doi:10.1111/apha.13460

35. Mehlem A, Hagberg CE, Muhl L, Eriksson U, Falkevall A. Imaging of neutral lipids by oil red O for analyzing the metabolic status in health and disease. *Nat Protoc*. 2013;8(6):1149-1154. doi:10.1038/nprot.2013.055

36. Folch J, Lees M, Sloane Stanley GH. A simple method for the isolation and purification of total lipides from animal tissues. *J Biol Chem*. 1957;226(1):497-509. doi:10.1016/s0021-9258(18)64849-5

37. Stout MB, Liu LF, Belury MA. Hepatic steatosis by dietary-conjugated linoleic acid is accompanied by accumulation of diacylglycerol and increased membrane-associated protein kinase C ε in mice. *Mol Nutr Food Res*. 2011;55(7):1010-1017. doi:10.1002/mnfr.201000413

38. Harrison KA, Bergman BC. HPLC-MS/MS methods for diacylglycerol and sphingolipid molecular species in skeletal muscle. In: *Methods in Molecular Biology*. Vol 1978. Humana, New York, NY; 2019:137-152. doi:10.1007/978-1-4939-9236-2_9

39. Livak KJ, Schmittgen TD. Analysis of relative gene expression data using real-time quantitative PCR and the 2-ΔΔCT method. *Methods*. 2001;25(4):402-408. doi:10.1006/meth.2001.1262

40. Batushansky A, Matsuzaki S, Newhardt MF, West MS, Griffin TM, Humphries KM. GC–MS metabolic profiling reveals fructose-2,6-bisphosphate regulates branched chain amino acid metabolism in the heart during fasting. *Metabolomics*. 2019;15(2):18. doi:10.1007/s11306-019-1478-5

41. Wolff CA, Lawrence MM, Porter H, et al. Sex differences in changes of protein synthesis with rapamycin treatment are minimized when metformin is added to rapamycin. *Geroscience*. Published online 2020. doi:10.1007/s11357-020-00243-8

42. Konopka AR, Laurin JL, Musci R v., et al. Influence of Nrf2 activators on subcellular skeletal muscle protein and DNA synthesis rates after 6 weeks of milk protein feeding in older adults. *Geroscience*. 2017;39(2):175-186. doi:10.1007/s11357-017-9968-8

43. Miller BF, Baehr LM, Musci R v., et al. Muscle-specific changes in protein synthesis with aging and reloading after disuse atrophy. *J Cachexia Sarcopenia Muscle*. 2019;10(6):1195-1209. doi:10.1002/jcsm.12470

44. Miller BF, Robinson MM, Bruss MD, Hellerstein M, Hamilton KL. A comprehensive assessment of mitochondrial protein synthesis and cellular proliferation with age and caloric restriction. *Aging Cell*. 2012;11(1):150-161. doi:10.1111/j.1474-9726.2011.00769.x

45. Miller BF, Robinson MM, Reuland DJ, et al. Calorie restriction does not increase short-term or long-term protein synthesis. *Journals of Gerontology - Series A Biological Sciences and Medical Sciences*. 2013;68(5):530-538. doi:10.1093/gerona/gls219

46. Kobak KA, Lawrence MM, Pharaoh G, et al. Determining the contributions of protein synthesis and breakdown to muscle atrophy requires non-steady-state equations. *J Cachexia Sarcopenia Muscle*. 2021;12(6):1764-1775. doi:10.1002/jcsm.12772

47. Kinter M, Sherman NE. *Protein Sequencing and Identification Using Tandem Mass Spectrometry*. John Wiley & Sons, Inc.; 2000. doi:10.1002/0471721980

48. R Core Team. R: A language and environment for statistical computing. Published online 2020.

49. Leys C, Ley C, Klein O, Bernard P, Licata L. Detecting outliers: Do not use standard deviation around the mean, use absolute deviation around the median. *J Exp Soc Psychol*. 2013;49(4):764-766. doi:10.1016/j.jesp.2013.03.013

50. Sud M, Fahy E, Cotter D, et al. LMSD: LIPID MAPS structure database. *Nucleic Acids Res*. 2007;35(suppl_1):D527-D532. doi:10.1093/NAR/GKL838

51. Multivariate data analysis. Accessed April 18, 2023. https://scienceinside.shinyapps.io/mvda/

52. Poret JM, Souza-Smith F, Marcell SJ, et al. High fat diet consumption differentially affects adipose tissue inflammation and adipocyte size in obesity-prone and obesity-resistant rats. *Int J Obes*. 2018;42(3):535-541. doi:10.1038/ijo.2017.280

53. Mei M, Zhao L, Li Q, et al. Inflammatory stress exacerbates ectopic lipid deposition in C57BL/6J mice. *Lipids Health Dis*. 2011;10(1):1-10. doi:10.1186/1476-511X-10-110/FIGURES/5

54. Sachs S, Zarini S, Kahn DE, et al. Intermuscular adipose tissue directly modulates skeletal muscle insulin sensitivity in humans. *Am J Physiol Endocrinol Metab*. 2019;316:866-879. doi:10.1152/ajpendo.00243.2018.-Intermuscular

55. Jani S, da Eira D, Hadday I, et al. Distinct mechanisms involving diacylglycerol, ceramides, and inflammation underlie insulin resistance in oxidative and glycolytic muscles from high fat-fed rats. *Sci Rep*. 2021;11(1):19160. doi:10.1038/s41598-021-98819-7

56. Bergman BC, Hunerdosse DM, Kerege A, Playdon MC, Perreault L. Localisation and composition of skeletal muscle diacylglycerol predicts insulin resistance in humans. *Diabetologia*. 2012;55(4):1140-1150. doi:10.1007/s00125-011-2419-7

57. Krogh-Madsen R, Plomgaard P, Møller K, Mittendorfer B, Pedersen BK. Influence of TNF-α and IL-6 infusions on insulin sensitivity and expression of IL-18 in humans. *Am J Physiol Endocrinol Metab*. 2006;291(1). doi:10.1152/ajpendo.00471.2005

58. Tchoukalova YD, Koutsari C, Votruba SB, et al. Sex- and depot-dependent differences in adipogenesis in normal-weight humans. *Obesity*. 2010;18(10):1875-1880. doi:10.1038/oby.2010.56

59. Zhou G, Myers R, Li Y, et al. Role of AMP-activated protein kinase in mechanism of metformin action. *J Clin Invest*. 2001;108(8):1167-1174. doi:10.1172/JCI13505

60. Turban S, Stretton C, Drouin O, et al. Defining the contribution of AMP-activated protein kinase (AMPK) and protein kinase C (PKC) in regulation of glucose uptake by metformin in skeletal muscle cells. *J Biol Chem*. 2012;287(24):20088-20099. doi:10.1074/JBC.M111.330746

61. Bailey CJ, Puah JA. Effect of metformin on glucose metabolism in mouse soleus muscle. *Diabete Metab*. 1986;12(4):212-218. Accessed March 9, 2023. https://europepmc.org/article/med/3770275

62. Ichael M, Tumvoll S, Abriele G, et al. Metabolic Effects of Metformin in Non-Insulin-Dependent Diabetes Mellitus. *https://doi.org/101056/NEJM199508313330903*. 1995;333(9):550-554. doi:10.1056/NEJM199508313330903

63. Newsom SA, Miller BF, Hamilton KL, Ehrlicher SE, Stierwalt HD, Robinson MM. Long-term rates of mitochondrial protein synthesis are increased in mouse skeletal muscle with high-fat feeding regardless of insulin-sensitizing treatment. *Am J Physiol Endocrinol Metab*. 2017;313:552-562. doi:10.1152/ajpendo.00144.2017.-Skeletal

64. Chanseaume E, Giraudet C, Gryson C, et al. Enhanced Muscle Mixed and Mitochondrial Protein Synthesis Rates after a High-fat or High-sucrose Diet. *Obesity*. 2007;15(4):853-859. doi:10.1038/OBY.2007.582

65. Ehrlicher SE, Stierwalt HD, Miller BF, Newsom SA, Robinson MM. Mitochondrial adaptations to exercise do not require Bcl2-mediated autophagy but occur with BNIP3/Parkin activation. *FASEB Journal*. 2020;34(3):4602-4618. doi:10.1096/fj.201902594RR

66. Dasari S, Newsom SA, Ehrlicher SE, Stierwalt HD, Robinson MM. Remodeling of skeletal muscle mitochondrial proteome with high-fat diet involves greater changes to β-oxidation than electron transfer proteins in mice. *Am J Physiol Endocrinol Metab*. 2018;315(4):E425-E434. doi:10.1152/AJPENDO.00051.2018/SUPPL_FILE/PROTEIN

67. Razmara A, Sunday L, Stirone C, et al. Mitochondrial Effects of Estrogen Are Mediated by Estrogen Receptor α in Brain Endothelial Cells. *Journal of Pharmacology and Experimental Therapeutics*. 2008;325(3):782-790. doi:10.1124/jpet.107.134072

68. O'Lone R, Knorr K, Jaffe IZ, et al. Estrogen receptors α and β mediate distinct pathways of vascular gene expression, including genes involved in mitochondrial electron transport and generation of reactive oxygen species. *Molecular Endocrinology*. 2007;21(6):1281-1296. doi:10.1210/me.2006-0497

69. Hevener AL, Ribas V, Moore TM, Zhou Z. The Impact of Skeletal Muscle ERα on Mitochondrial Function and Metabolic Health. *Endocrinology*. 2020;161(2):1-16. doi:10.1210/endocr/bqz017

70. Ribas V, Drew BG, Zhou Z, et al. Skeletal muscle action of estrogen receptor a is critical for the maintenance of mitochondrial function and metabolic homeostasis in females. *Sci Transl Med*. 2016;8(334):334ra54-334ra54. doi:10.1126/scitranslmed.aad3815

Figure Legends

Figure 1: Study design schematic. To understand the effects of 17α-E2 on skeletal muscle in response to a metabolic challenge, male and female mice (3-months) were fed a 45% high-fat diet (HFD). Additionally, male and female (n = 10 and n = 10, respectively) groups of age-matched WT, mice were given a chow diet to act as controls. All mice (age: 12 months) on HFD were randomized into HFD or HFD+17α-E2 (n = 7-10/sex/group) treatment groups for a 3.5-month intervention. All mice underwent deuterium oxide (D_2O) stable isotope labeling during the last 10 days of the intervention to determine changes to the skeletal muscle myofibrillar and mitochondrial fractions.

Figure 2: Phenotype description of groups from chow (black), HFD (red), and HFD+17α-E2 (blue). **A-F**) Body composition measures for male (**A-C**) and female mice (**D-F**). Data were analyzed by two-way ANOVA (Treatment x Time) and data are in mean ± SEM from 7–10 mice per group. *p < 0.05 between HFD and HFD+17α-E2, †p < 0.05 between HFD and Chow, ‡p < 0.05 between HDF+17α-E2 and Chow. “a”, “b”, and “c” indicate which timepoint became significantly different (p < 0.05) from week 0 within HFD, HFD+17α-E2, and Chow, respectively. **G**) Lean mass percentage in male and female mice. **H-K**) Skeletal muscle weights normalized to body mass. (**G-K**) Data were analyzed by one-way ANOVA, data are in mean ± SEM from 7–10 mice per group, *p < 0.05, **p < 0.01, ***p < 0.001, and ****p < 0.0001.

Figure 3: Results for p-AKT:AKT, p-4E-BP1:4E-BP1, p-S6:S6, and p-AMPKα:AMPKα ratios in **A**) male and **B**) female mice, respectively. Representative blots of p-AKT, AKT, p-S6, S6, 4E-BP1, p-4E-BP1, p-AMPKα, and AMPKα from Chow, HFD, and HFD+17α-E2. Data are expressed as mean ± SEM of 6–10 mice per treatment group and were analyzed by one-way ANOVA, *p < 0.05 and **p < 0.01.

Figure 4: A) Concentration of triacyclglycerols in the quadriceps muscle. **B**) Oil-red-O staining intensity in gastrocnemius in arbitrary units (a.u). **C**) Representative images of Oil-Red-O stain. **D**) Total 1,2-DAGs and 1,3-DAG content of the gastrocnemius muscle. **E**) Individual 1,2-DAGs represented as fold change from Chow. All lipids shown are significantly different in male and/or female mice. *p < 0.05, **p < 0.01, ***p < 0.001, and

****p < 0.0001. Values are in mean ± SEM from 7–10 mice per treatment group and were analyzed by one-way ANOVA.

Figure 5: A) mRNA expression of inflammatory cytokines in the TA muscle. **B**) The pro-inflammatory cytokine and chemokine protein concentrations in the plantaris muscle. Values are in mean ± SEM from 7–10 mice per treatment group and were analyzed by one-way ANOVA,*p < 0.05, **p < 0.01, and ****p < 0.0001.

Figure 6: PCA plots for metabolite abundance in **A**) male and **B**) female mice. Relative abundance of amino acid content in gastrocnemius of **C**) male and **D**) female mice. Values are in mean ± SEM from 7–10 mice per treatment group and were analyzed by one-way ANOVA,*p < 0.05, **p < 0.01, ***p < 0.001, and ****p < 0.0001.

Figure 6: PCA plots for metabolite abundance in **A**) male and **B**) female mice. Relative abundance of amino acid content in gastrocnemius of **C**) male and **D**) female mice. Values are in mean ± SEM from 7–10 mice per treatment group and were analyzed by one-way ANOVA,*p < 0.05, **p < 0.01, ***p < 0.001, and ****p < 0.0001.

Figure 7: A) Myofibrillar and **B**) mitochondrial fraction synthesis rates (%/Day). PCA for **C**) males and **D**) female mice. Volcano plot representing the relative difference in protein abundance between HFD+17α-E2 and HFD of **E**) male and **F**) female mice. These data are from 7–10 mice per treatment group and were analyzed by one-way ANOVA, *p < 0.05, **p < 0.01, and ***p < 0.001.

Figures

Figure 1

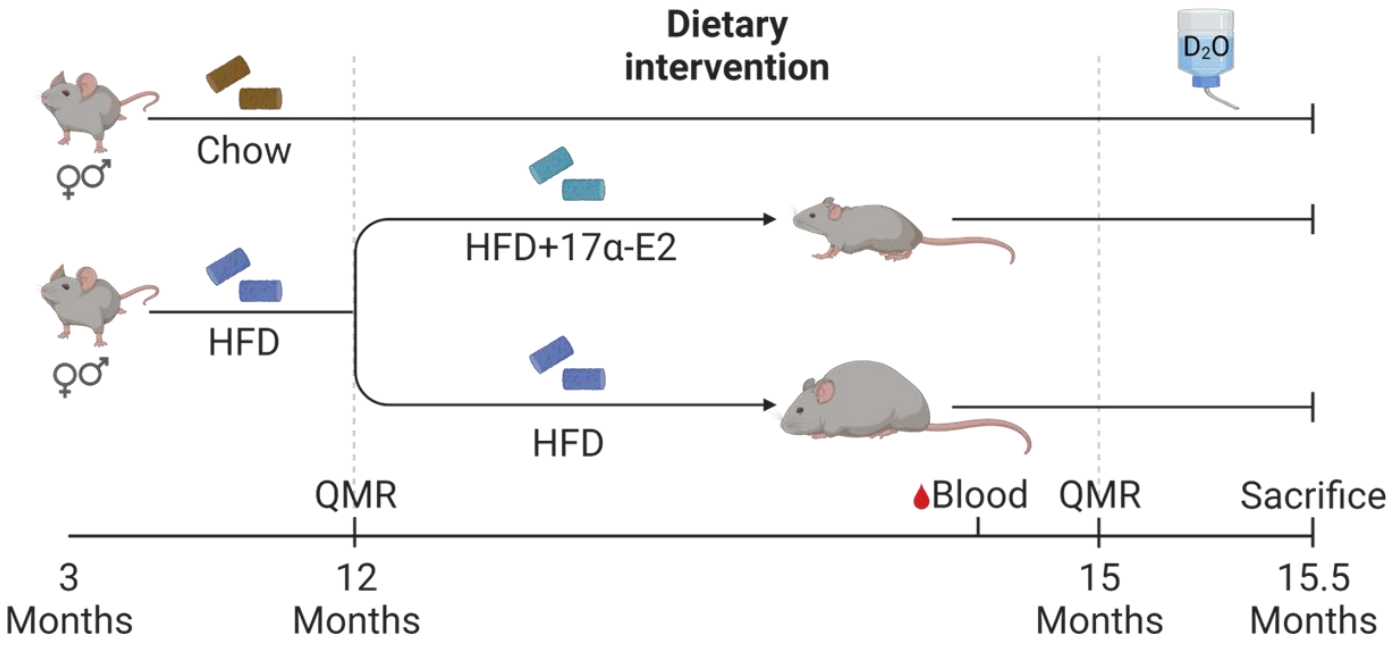

Figure 2

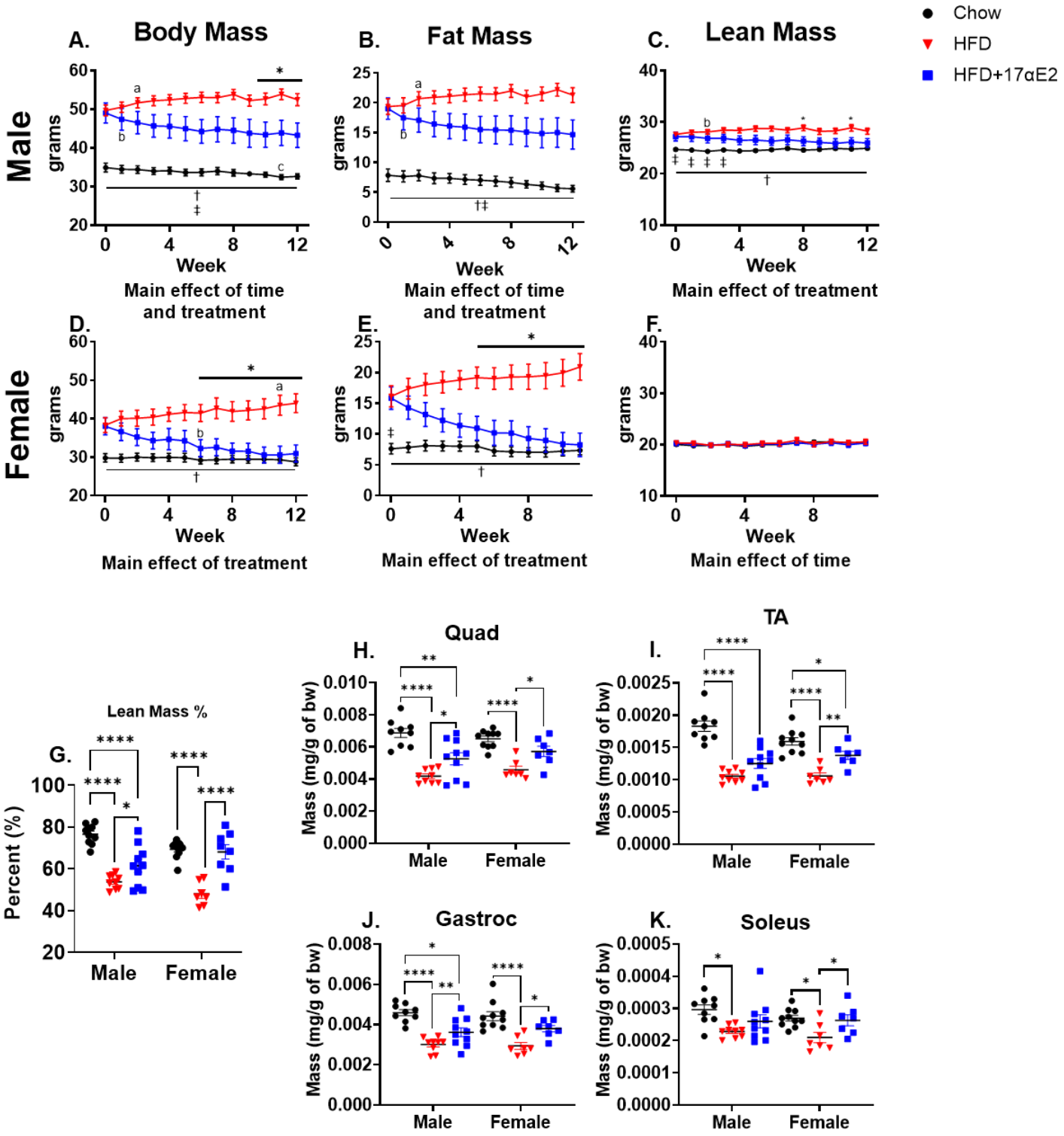
Chow
HFD
HFD+17αE2
Male
Female
A. Body Mass
B. Fat Mass
C. Lean Mass
D.
E.
F.
grams
Week
Main effect of time and treatment
Main effect of treatment
Main effect of time
Lean Mass %
G.
Percent (%)
Male
Female
Quad
H.
TA
I.
Gastroc
J.
Soleus
K.
Mass (mg/g of bw)

Figure 3

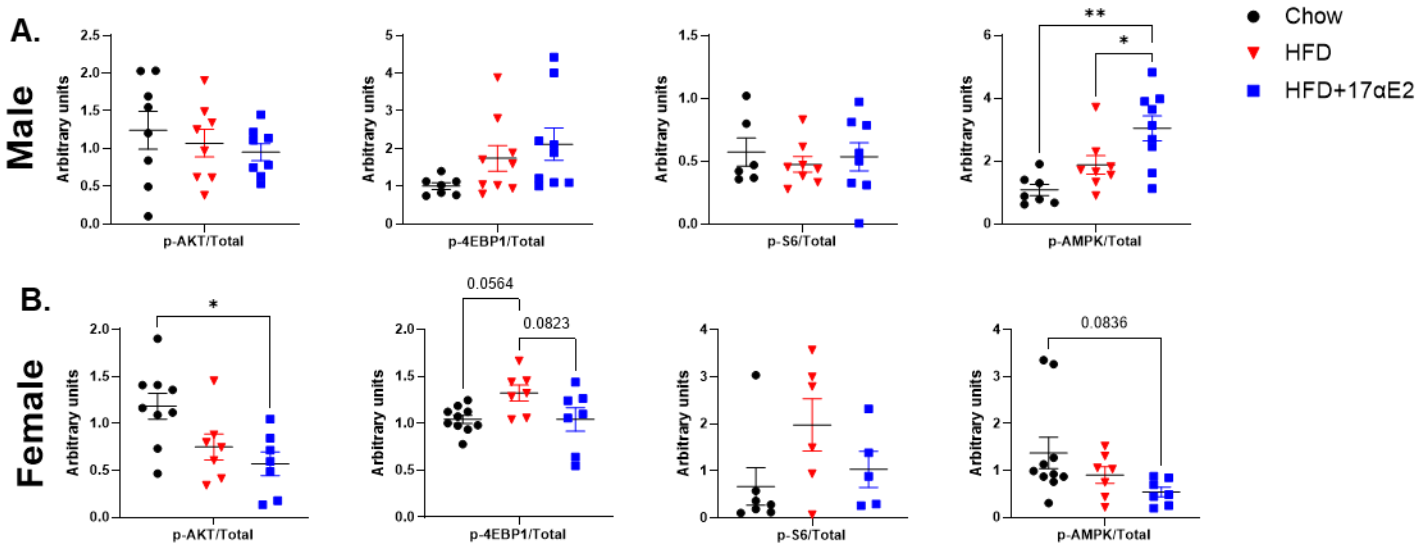
A.
Male
Arbitrary units
p-AKT/Total
p-4EBP1/Total
p-S6/Total
p-AMPK/Total
**
*
Chow
HFD
HFD+17αE2
B.
Female
*
0.0564
0.0823
0.0836

Figure 4

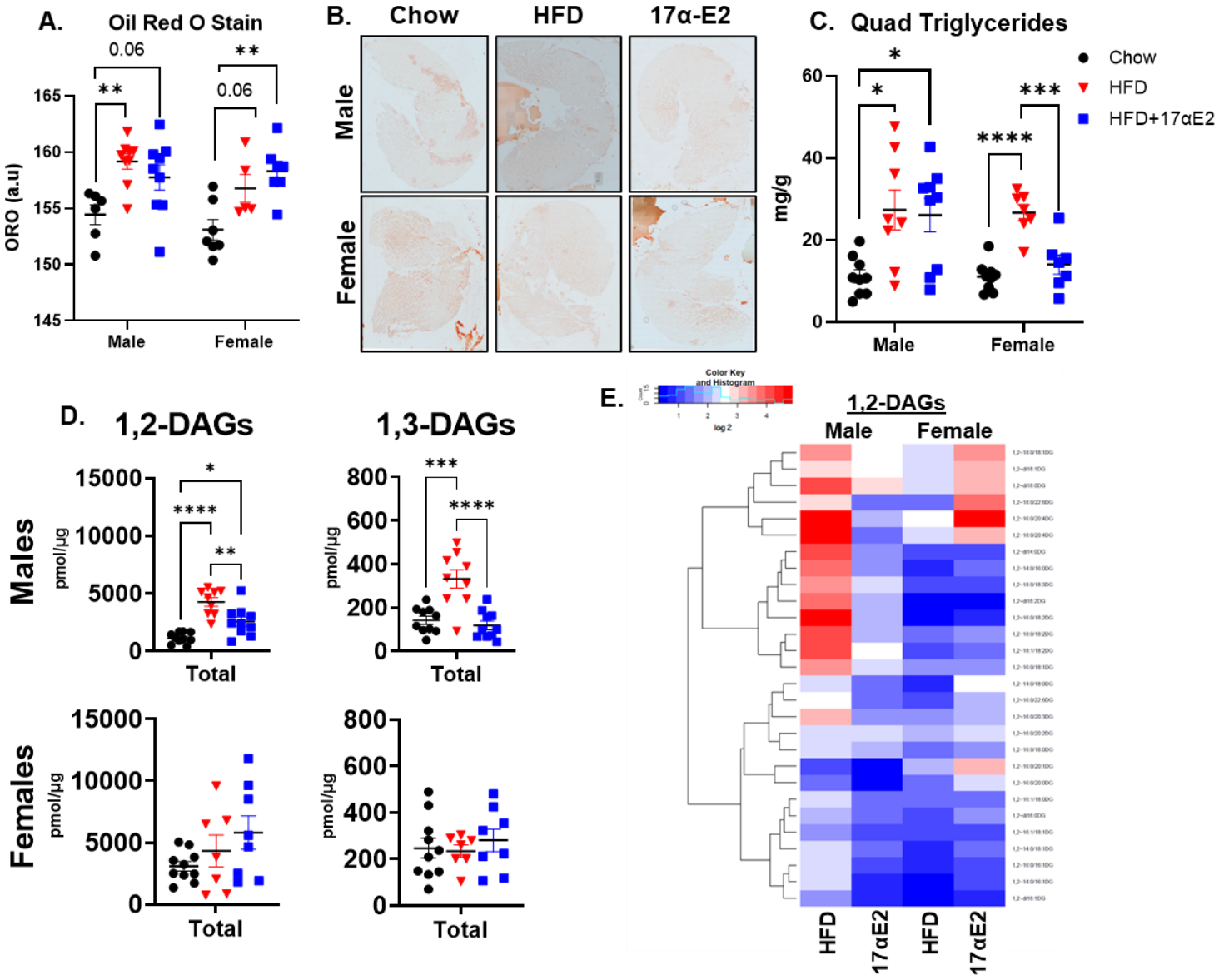
A.
Oil Red O Stain
0.06
**
**
0.06
ORO (a.u)
165
160
155
150
145
Male
Female
B.
Chow
HFD
17α-E2
Male
Female
C.
Quad Triglycerides
Chow
HFD
HFD+17αE2
mg/g
60
40
20
0
*
*
***
****
Male
Female
D.
1,2-DAGs
1,3-DAGs
Males
Females
pmol/µg
15000
10000
5000
0
800
600
400
200
0
*
****
**
***
****
Total
E.
Color Key and Histogram
log 2
1,2-DAGs
Male
Female
HFD
17αE2
HFD
17αE2

Figure 5

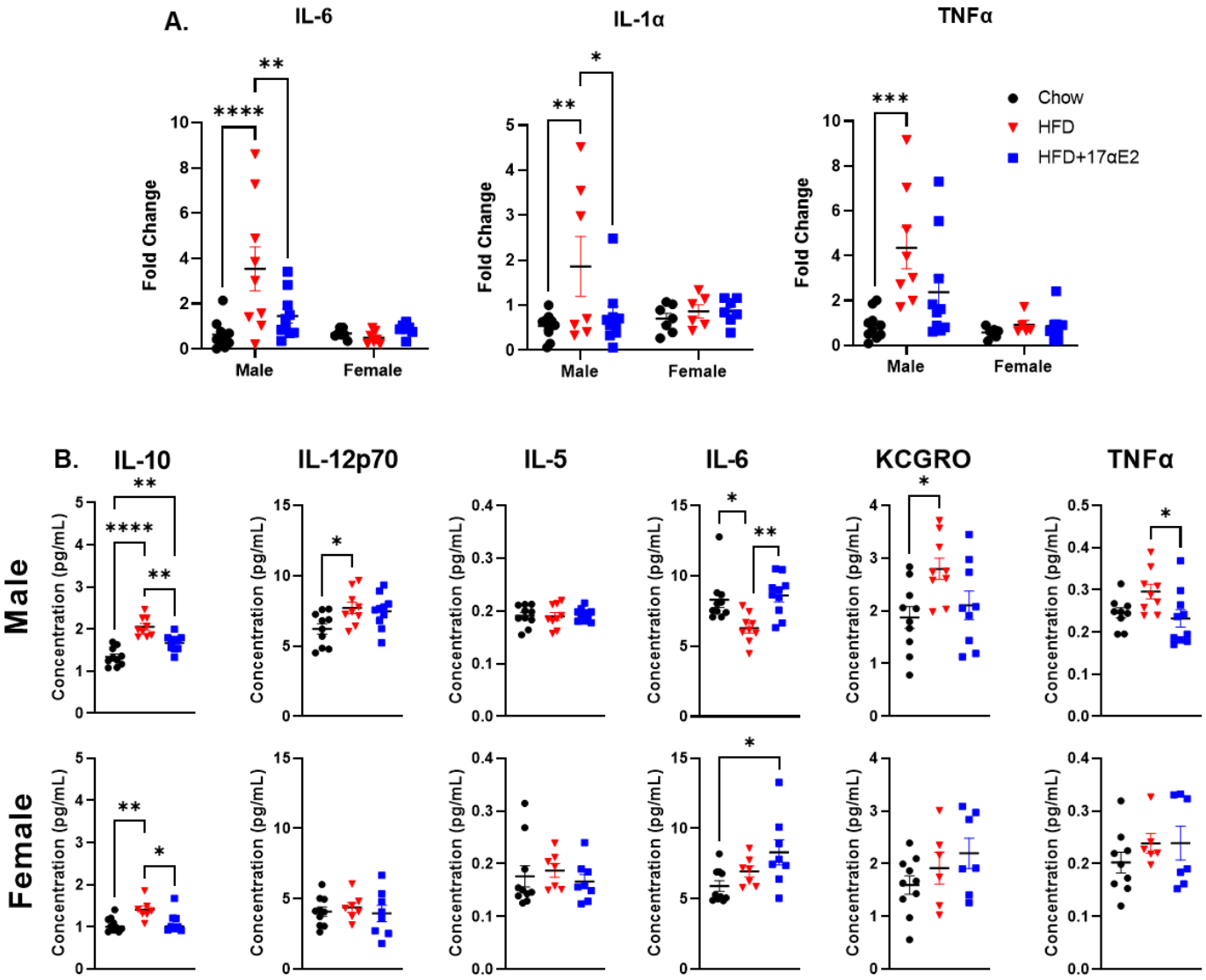
A.
IL-6
IL-1α
TNFα
Fold Change
Male
Female
Chow
HFD
HFD+17αE2
B.
IL-10
IL-12p70
IL-5
IL-6
KCGRO
TNFα
Male
Female
Concentration (pg/mL)

Figure 6

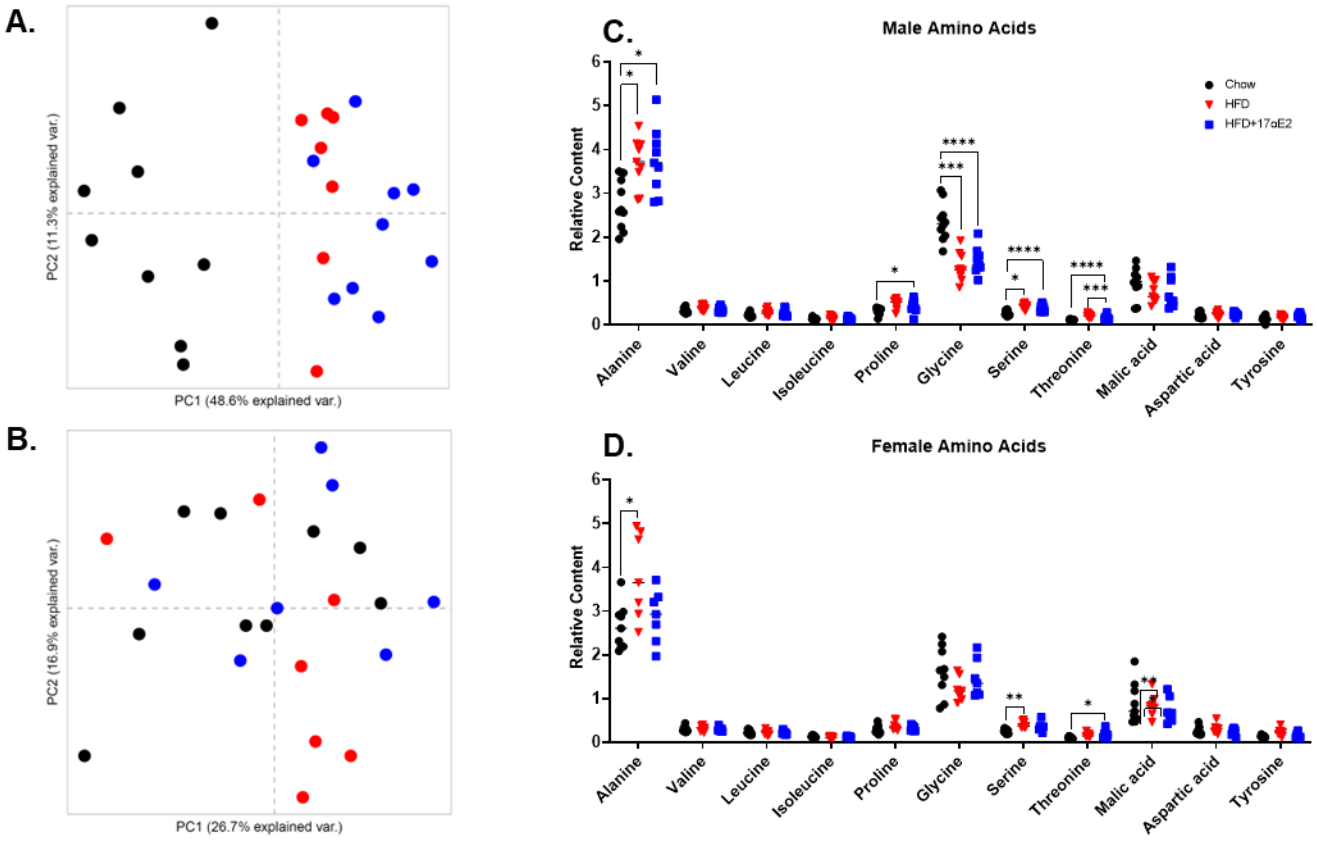
A.
PC2 (11.3% explained var.)
PC1 (48.6% explained var.)
B.
PC2 (16.9% explained var.)
PC1 (26.7% explained var.)
C.
Male Amino Acids
Relative Content
Chow
HFD
HFD+17αE2
Alanine
Valine
Leucine
Isoleucine
Proline
Glycine
Serine
Threonine
Malic acid
Aspartic acid
Tyrosine
D.
Female Amino Acids
Relative Content
Alanine
Valine
Leucine
Isoleucine
Proline
Glycine
Serine
Threonine
Malic acid
Aspartic acid
Tyrosine

Figure 7

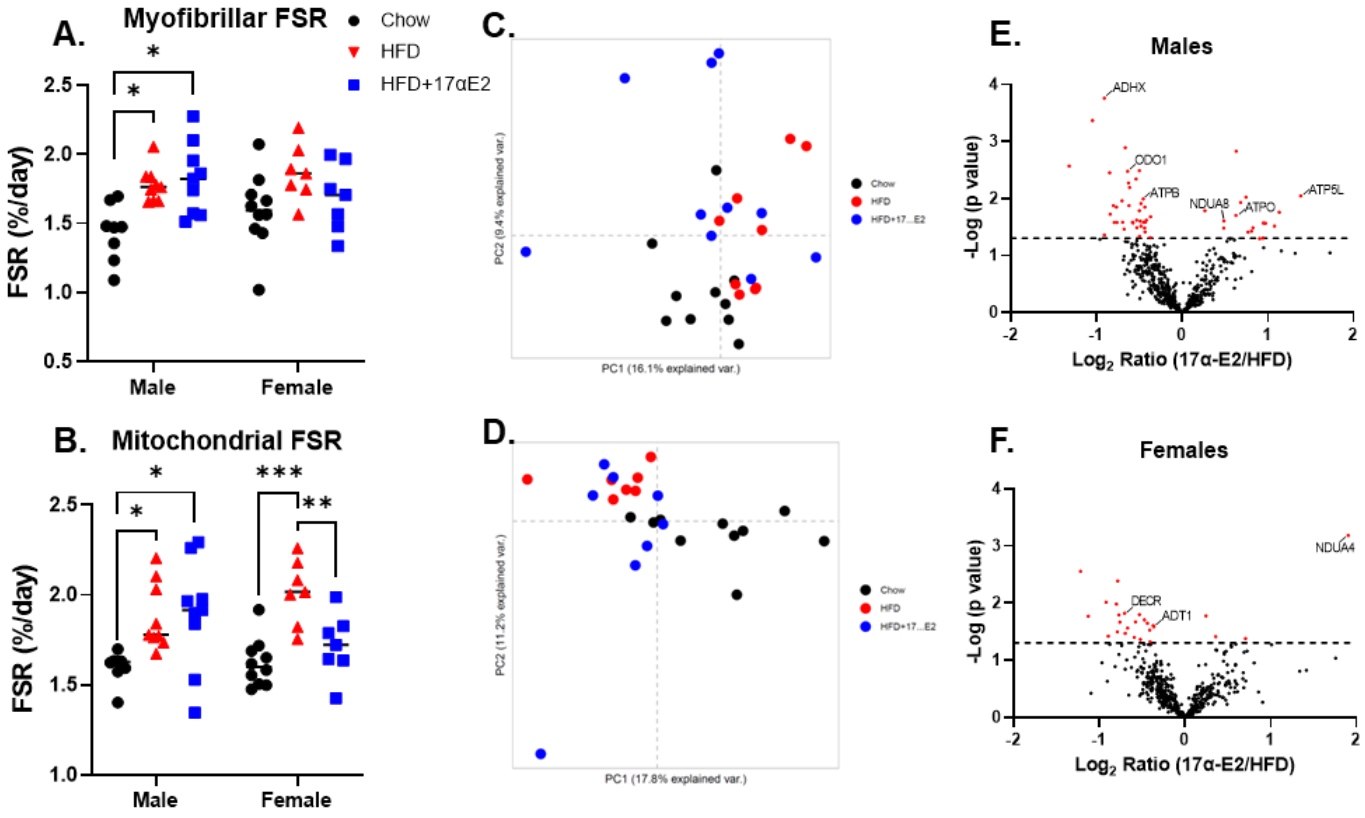
A.
Myofibrillar FSR
Chow
HFD
HFD+17αE2
FSR (%/day)
Male
Female
B.
Mitochondrial FSR
FSR (%/day)
Male
Female
C.
PC1 (16.1% explained var.)
PC2 (9.4% explained var.)
D.
PC1 (17.8% explained var.)
PC2 (11.2% explained var.)
E.
Males
-Log (p value)
Log2 Ratio (17α-E2/HFD)
ADHX
CDO1
ATPB
NDUA8
ATPO
ATP5L
F.
Females
-Log (p value)
Log2 Ratio (17α-E2/HFD)
NDUA4
DECR
ADT1